

Photoacid for Extremely Long-Lived and Reversible pH-Jumps

Rui M. D. Nunes, Marta Pineiro,* and Luis G. Arnaut*

Chemistry Department, University of Coimbra, 3000 Coimbra, Portugal

Received March 18, 2009; E-mail: mpineiro@qui.uc.pt

Abstract: The ability to change the acidity of an aqueous solution within the time of a short laser pulse and use the resulting low pH to drive acid-catalyzed reactions in the irradiated volume opens new perspectives for the spatial and temporal control of a variety of processes. Persistent and reversible acidification of an aqueous solution is achieved with a new molecule, 1-(2-nitroethyl)-2-naphthol, that combines the fast photoacid properties of an aromatic alcohol with the slow proton transfer rates of a nitroalkane. The protons released in a few nanoseconds by pulsed laser excitation of the photoacid last for nearly one second in aqueous solutions. We show that acid–base equilibria with other species is established at the lower pHs of the irradiated volume, that the process is reversible and that it can be maintained under continuous irradiation.

1. Introduction

Aromatic alcohols, such as naphthols, become strong acids when they absorb light.¹ Their enhanced acidity in the excited state is reasonably well predicted by the Förster equation

$$pK_a^* = pK_a - (\nu_{HA} - \nu_{A^-})/2.3RT \quad (1)$$

where $h\nu_{HA(A^-)}$ is the energy of the 0–0 electronic transition for the conjugated acid (base). In addition to a decrease in 6–8 pK_a units upon electronic excitation, such photoacids also transfer very rapidly a proton to a nearby water molecule and are capable of transforming a neutral aqueous solution into an acidic one within nanoseconds.

The acidification of a solution with a photoacid and a short laser pulse can be used to perturb rapid acid–base equilibria and to initiate acid-catalyzed reactions in less than 10 ns, which are of interest to uncover mechanisms of acid–base catalysis,² study the initial steps of protein folding³ or phototrigger liposomal drug delivery.⁴ Moreover, the spatial control of pH in the nanoscale can be exploited for photolithography,⁵ and for mechanistic studies in confined (subcellular,⁶ nanostructured) volumes. Indeed, the features obtained by photolithography in the semiconductor industry now approach 100 nm and even considering the abnormally large value for the proton diffusion coefficient in water, $D = 9.3 \text{ nm}^2/\text{ns}$ at 300 K,⁷ the translation distance $R_t = \sqrt{2Dt} = 100 \text{ nm}$ is only accessed in 550 ns. The duration of the pH jump must be sufficiently longer

than this to ensure that the nanometric features are controlled by the kinetics of the acid-catalyzed reaction with the substrate. Furthermore, it is practical to focus a laser beam to a diameter below 1 μm , which is comparable to the sizes of cellular organelles of most Eukaryotic animal cells. However, these potential applications require the stabilization of the pH drop in the irradiated volume within a nanosecond laser pulse, the maintenance of the acidity for orders of magnitude longer time scales and the absence of contamination by side products. The ideal photoacid should have a $pK_a > 8$ and a low pK_a^* (< 2), deprotonate in a few nanoseconds in aqueous solutions upon electronic excitation and reversibly reprotonate very slowly. A strong, persistent and reversible photoacid would meet the specifications for the applications mentioned above.

The fast production of an acidic solution using a short laser pulse attracted much interest over the last 30 years. This was the original aim of the pH jump experiment, which employed naphthol derivatives.⁸ However, the conjugated bases of these photoacids rapidly return to the electronic ground state, where they reprotonate and neutralize the solutions in hundreds of nanoseconds.⁹ The bimolecular reprotonation rate increases with the concentration of the conjugated base and limits naphthols to the generation of small and short-lived pH jumps. Much larger pH jumps have been achieved with the introduction of “super” photoacids, with negative pK_a^* s,^{10,11} but this did not solve the problem of the fast reprotonation of the conjugated base. Alternatively, longer-lived pH jumps are produced when a proton is released from a photolabile “caging” group.^{12,13}

(1) Arnaut, L. G.; Formosinho, S. J. *J. Photochem. Photobiol. A: Chem.* **1993**, *75*, 1–20.

(2) Politi, M. J.; Fendler, J. H. *J. Am. Chem. Soc.* **1984**, *26*, 5–273.

(3) Abbruzzetti, S.; Crema, E.; Masino, L.; Vecchi, A.; Viappiani, C.; Small, J. R.; Libertini, L. J.; Small, E. W. *Biophys. J.* **2000**, *78*, 405–415.

(4) Shum, P.; Kim, J.-M.; Thompson, D. H. *Adv. Drug Delivery Rev.* **2001**, *53*.

(5) Wallraff, G. M.; Hinsberg, W. D. *Chem. Rev.* **1999**, *99*, 1801–1821.

(6) Fraser, J. A.; Middlebrook, C. E.; Usher-Smith, J. A.; Schwiening, C. J.; Huang, C. L. H. *J. Physiol.* **2005**, *563*, 745–764.

(7) Agmon, N. *Isr. J. Chem.* **1999**, *39*, 493–502.

(8) Gutman, M.; Huppert, D. *J. Biochem. Biophys. Methods* **1979**, *1*, 9–19.

(9) Gutman, M.; Nachliel, E.; Gershon, E.; Giniger, R.; Pines, E. *J. Am. Chem. Soc.* **1983**, *105*, 2210–2216.

(10) Tolbert, L. M.; Haubrich, J. E. *J. Am. Chem. Soc.* **1994**, *116*, 10593–10600.

(11) Tolbert, L. M.; Solntsev, K. M. *Acc. Chem. Res.* **2002**, *35*, 19–27.

(12) Bonetti, G.; Vecchi, A.; Viappiani, C. *Chem. Phys. Lett.* **1997**, *269*, 268–273.

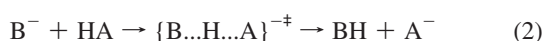
(13) Barth, A.; Corrie, J. E. T. *Biophys. J.* **2002**, *83*, 2864–2871.

Photoactivation of such compounds initiates a series of reactions where one of the intermediates is a strong acid that deprotonates and rapidly converts into a photolysis product with low pK_a .¹⁴ With such caged proton compounds, the size of the pH jump is limited by the pK_a of the photolysis product and the irreversibility is a source of contamination.

The advances in the pH jump technique have been insufficient to promote it as a general tool to perturb acid–base equilibria or to induce acid-catalyzed reactions. Further progress requires a reversible photoacid capable of acidifying persistently its aqueous environment when irradiated with a single laser pulse. In this work we develop the concept of persistent and reversible photoacids using Formosinho's Interacting-State Model (ISM)^{15–17} and its applications to proton transfers in solution and in enzymes.^{16,18} ISM is employed to design the structure of a photoacid capable of very fast excited-state deprotonation and very slow ground-state reprotonation. It is shown that this can be achieved with naphthol derivatives provided that intramolecular proton transfer from an activated carbon acid is made competitive with the excited-state decay of the naphtholate. ISM calculations show that one nitro group is sufficient for this purpose if the acidic proton closes a 6-membered ring with the oxygen atom of the naphtholate. These predictions motivated the synthesis of 1-(2-nitroethyl)-2-naphthol (NO2nH). We show that aqueous solutions of this molecule remain acidic under continuous irradiation, reversibly retuning to neutrality in the dark. On–off light cycles generate acid-neutral pH cycles, each lasting for approximately one second. The reversibility of the system supports the operation of a molecular proton pump driven by light. Using intense and focused laser beams, it becomes possible to control acidity in the nanoscale within nanoseconds.

2. Theoretical Design

ISM has been described in detail in various recent publications,^{16,17,19} including applications to proton transfer reactions in solution^{16,20} and in enzymes.^{18,21} Briefly, the classical reaction path of ISM for the general proton transfer reaction



is a linear interpolation between the Morse curves of HA and HB along the reaction coordinate

$$V_{cl}(n) = (1 - n)V_{HA} + nV_{HB} + n\Delta V^0 \quad (3)$$

where n is the HB bond order and the classical reaction energy is

$$\Delta V^0 = -RT(2.303pK_{HA} + \ln(p_A/q_A) - 2.303pK_{HB} - \ln(p_B/q_B)) - Z_{HA} + Z_{HB} \quad (4)$$

pK_{AH} and pK_{BH} are the thermodynamic acidity constants of AH and BH, p_A (p_B) is the number of equivalent protons in AH (BH), q_A (q_B) is the number of equivalent basic sites in AH (BH), and Z_{AH} (Z_{BH}) is the zero-point energy of the AH (BH) bond. The presence of hydrogen-bonded intermediates is included in this reaction path using the Lippincott-Schroeder potential.²² Zero-point energies are added to the classical reaction coordinate of ISM and the resulting vibrationally adiabatic path is employed to calculate rate constants using the semiclassical transition state theory. Intramolecular proton transfers are treated in the same way, except that the entropy lost in attaining the six-membered ring may be taken from that of cyclohexane, $\Delta^\ddagger S = -18.8 \text{ cal mol}^{-1} \text{ K}^{-1}$,²³ and included in the pre-exponential factor. Details are given in the Supporting Information. The calculations were run in the freely available Internet application,^{16b} uploading the input files presented in the Supporting Information. The output files are also presented in the Supporting Information.

Figure 1 presents the rates of the proton transfer cycle calculated with ISM based on known pK_a values of analogous compounds, $pK_a(2\text{-naphthol}) = 9.45$ ¹⁰ and $pK_a(2\text{-nitro-ethyl-benzene}) = 8.78$ in water and 9.82 in 50% MeOH/H₂O,²⁴ respectively. ISM predicts that intramolecular quenching of the electronically excited naphtholate ion by an acidic proton of a nitroalkane moiety is competitive with its nanosecond lifetime. For example, the anion derived from 1-propyl-2-naphthol has an excited state decay with a major component *ca.* $5 \times 10^7 \text{ s}^{-1}$,²⁵ whereas the calculated intramolecular proton transfer rate constant from the acidic carbon to RO[−] is $k_{ipt} = 2.6 \times 10^8 \text{ s}^{-1}$. Thus, we expect that 80% of the naphtholate fluorescence is quenched by nonadiabatic intramolecular proton transfer to yield a ground-state carbanion located at the α position to the nitro group. This carbanion is trapped in a deep potential well, with a barrier of 7 kcal/mol preventing its protonation by the oxonium ion and a barrier of 14 kcal/mol in the way of the ground-state intramolecular proton transfer from the naphthol moiety.

The intramolecular proton transfer neutralizes the naphtholate but generates a carbanion next to a nitro group, which is recognized as the best carbanion-stabilizing group in organic chemistry.²⁶ ISM calculated rate constants for the protonation of this carbanion and for the deprotonation of the corresponding nitroalkane are $k_p = 5 \times 10^4$ and $k_d = 8 \times 10^{-7} \text{ M}^{-1} \text{ s}^{-1}$, respectively, but the deprotonation in water is more conveniently expressed as a first-order rate with $k_d[\text{H}_2\text{O}] \approx 4 \times 10^{-5} \text{ s}^{-1}$. The protonation of this carbanion is 10^6 times slower than that of ground-state 2-naphtholate, which is controlled by diffusion, and is expected to lead to pH jumps lasting one million times longer than those produced by naphthols.

The quantitative treatment of the carbanion reprotonation kinetics in a pH jump experiment must take into consideration that the return of the solution to neutrality is governed by the re-establishment of the equilibrium

- (14) Laimgruber, S.; Schreier, W. J.; Schrader, T.; Koller, F.; Zinth, W.; Gilch, P. *Angew. Chem., Int. Ed.* **2005**, *44*, 7901–7904.
 (15) Arnaut, L. G.; Pais, A. A. C. C.; Formosinho, S. J.; Barroso, M. *J. Am. Chem. Soc.* **2003**, *125*, 5236–5246.
 (16) (a) Barroso, M.; Arnaut, L. G.; Formosinho, S. J. *J. Phys. Chem. A* **2007**, *111*, 591–602. (b) <http://www.ism.qui.uc.pt:8180/ism/>.
 (17) Arnaut, L. G.; Formosinho, S. J. *Chem.—Eur. J.* **2008**, *14*, 6578–6587.
 (18) Barroso, M.; Arnaut, L. G.; Formosinho, S. J. *J. Phys. Org. Chem.* **2009**, *22*, 254–263.
 (19) Arnaut, L. G.; Formosinho, S. J. *Chem.—Eur. J.* **2007**, *13*, 8018–8028.
 (20) Arnaut, L. G.; Formosinho, S. J.; Barroso, M. *J. Mol. Struct.* **2006**, *786*, 207–214.
 (21) Barroso, M.; Arnaut, L. G.; Formosinho, S. J. *J. Phys. Org. Chem.* **2008**, *21*, 659–665.

- (22) Barroso, M.; Arnaut, L. G.; Formosinho, S. J. *ChemPhysChem* **2005**, *6*, 363–371.
 (23) Lowry, T. H.; Richardson, K. S., *Mechanism and Theory in Organic Chemistry*, 3rd ed.; Harper & Row Publishers: New York, 1987.
 (24) Bordwell, F. G.; Bartmess, J. E. *J. Org. Chem.* **1978**, *43*, 3101–3107.
 (25) Tolbert, L. M.; Harvey, L. C.; Lum, R. C. *J. Phys. Chem.* **1993**, *97*, 13335–13340.
 (26) Backstrom, N.; Burton, N. A.; Turega, S.; Watt, C. I. F. *J. Phys. Org. Chem.* **2008**, *21*, 603–613.



Under typical experimental conditions, $[\text{NO}_2\text{nH}]_0 \approx 10^{-4}$ M, $\text{p}K_a \approx 9$, pH 7, the relaxation time calculated with (6) is 2 seconds. The intramolecular carbanion protonation channel shown in Figure 1 also contributes to the relaxation time at millimolar photoacid concentrations, reducing it to *ca.* 1 s.

$$\tau = \frac{1}{k_p([\text{NO}_2\text{n}^-]_{\text{eq}} + [\text{H}^+]_{\text{eq}}) + k_d[\text{H}_2\text{O}]} \quad (6)$$

In summary, the ISM design of a persistent and reversible photoacid indicates that 1-(2-nitroethyl)-2-naphthol should deprotonate in the excited state within a nanosecond laser pulse to yield a carbanion competitively with a ground-state naphtholate, and that the carbanion may relax in one second back to neutrality.

3. Experimental Procedures

Materials. The reactants 2-hydroxynaphthalene-1-carbadehyde, nitromethane, *L*-proline, NaBH_4 and *o*-nitrobenzaldehyde were purchased from Aldrich. ^1H and ^{13}C NMR spectra were recorded in CDCl_3 solutions on Bruker Avance III de 400 MHz spectrometer.

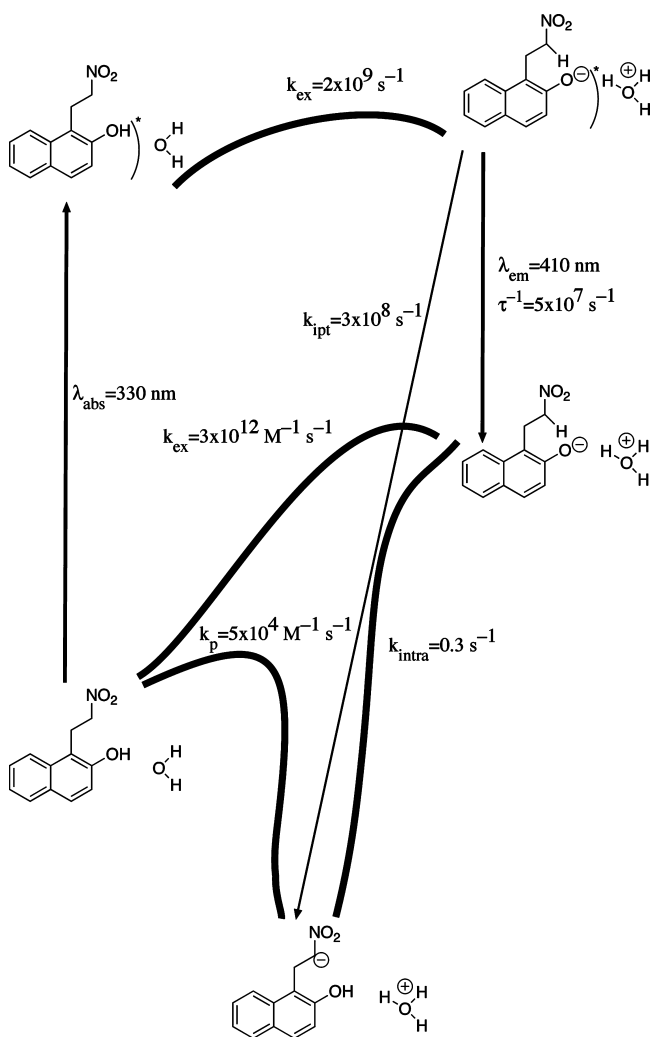


Figure 1. Energy landscape of NO_2nH according to ISM. It was assumed that $\text{p}K_a^*(\text{naphthol}) = 2$, $\text{p}K_a(\text{naphthol}) = 9.4$ and $\text{p}K_a(\text{nitroalkane}) = 9$ [see Supporting Information for the details of ISM calculations].

Potassium ferrioxalate actinometry was made according to standard procedures.^{27,28}

1-(2-Nitro-vinyl)-naphthalen-2-ol. 2-Hydroxynaphthalene-1-carbaldehyde (500 mg, 5.8 mmol), nitromethane (0.31 mL, 5.8 mmol) and *L*-proline (125 mg, 25%, w/w) were dissolved in 20 mL of methanol and heated at 50 °C. The reaction was followed by TLC until the reagents were undetectable. The reaction mixture was cooled to room temperature and the solvent evaporated. The reaction crude was dissolved in a mixture ether:dichloromethane (1:5, v/v) and warmed at 40 °C in a water bath until complete solubilization. Cooling to room temperature, 1-(2-nitro-vinyl)-naphthalen-2-ol precipitates as a solid in 17% yield.

1-(2-Nitro-ethyl)-naphthalen-2-ol (NO₂nH). 1-(2-Nitro-vinyl)-naphthalen-2-ol (250 mg, 1.2 mmol) was dissolved in 10 mL of a mixture of THF/methanol (1:10, v/v). Sodium borohydride was added, in portions to the stirring solution until the reaction mixture turned colorless. After quenched with water, the reaction mixture was extracted using dichloromethane/ $\text{NaCl}(\text{aq})$ at low temperature. After evaporation the dry product was obtained in 71% yield. In this work we employ the more trivial name 1-(2-nitroethyl)-2-naphthol for this molecule. ^1H NMR (400 MHz, CDCl_3) δ , ppm: 7.89(d, 1H, $J = 8.6$ Hz), 7.79(d, 1H, $J = 8.1$ Hz), 7.70(d, 1H, $J = 8.8$ Hz), 7.54(t, 1H, $J = 7.6$ Hz), 7.37(t, 1H, $J = 7.5$ Hz), 7.04(d, 1H, $J = 8.8$ Hz), 4.67(t, 1H, $J = 7.6$ Hz), 3.81(t, 1H, $J = 7.6$ Hz). ^{13}C NMR (400 MHz, CDCl_3) δ , ppm: 151.4, 132.9, 129.5, 129.4, 129.0, 127.4, 123.6, 121.8, 117.6, 113.6, 74.1, 19.7. MS (MALDI-TOF), m/z : 217 (M^+).

Methods. Absorption and luminescence spectra were recorded with Shimadzu UV-2100 and SPEX Fluoromax 3.22 spectrophotometers, respectively. Fluorescence lifetimes were measured with a previously described home-built time-correlated single-photon counting (SPC) apparatus using IBH nanoLEDs (281 nm) as excitation sources, Philips XP2020Q photomultiplier with excitation and emission wavelengths selected with Jobin-Ivon H20 monochromators, and a Canberra Instruments time-to-amplitude converter and multichannel analyzer.²⁹ Transient triplet-triplet absorption was obtained with an Applied Photophysics LKS.60 flash photolysis spectrometer with the R928 photomultiplier from Hamamatsu for detection and the HP Infinium (500 MHz, 1 GSa/s) or Tektronix DPO 7254 (2.5 GHz, 40 GSa/s) oscilloscopes. Excitation employed the fourth harmonic of a Spectra-Physics Quanta Ray GCR 130 Nd:YAG laser (5–6 ns pulse width). The energy per pulse was typically below 5 mJ at 266 nm.

4. Results and Discussion

The synthesis of 1-(2-nitroethyl)-2-naphthol, NO_2nH , was achieved through a Henry reaction using *L*-proline as catalyst,³⁰ and subsequent reduction with methanolic sodium borohydride.³¹ The negative influence of the hydroxyl group at the ortho position of the aldehyde in the Henry reaction was avoided using 2-benzyloxy-naphthalene-1-carbaldehyde. In fact, the corresponding condensation product, 2-benzyloxy-1-(2-nitrovinyl)-naphthalene, was obtained in 63% yield. The use of the aldehyde with the unprotected hydroxyl group in the condensation opens new routes for other reduction strategies for the carbon-carbon double bond, and gives us access to the desired product, although compromising the overall yield. Figure 2 shows the NMR spectrum of the molecule, with the triplet

(27) Hatchard, C. G.; Parker, C. A. *Proc. R. Soc.* **1956**, A235, 518.

(28) Arnaut, L. G.; Formosinho, S. J.; Burrows, H. D. *Chemical Kinetics*; Elsevier: Amsterdam, 2007; p 549.

(29) Melo, J. S.; Fernandes, P. F. *J. Mol. Struct.* **2001**, 69, 565.

(30) Kürti, L.; Czakov, B. *Strategic applications of named reactions in organic synthesis*; Elsevier Academic Press: London, 2005.

(31) Varma, R. S.; Kabalka, G. W. *Synth. Commun.* **1985**, 15, 151.

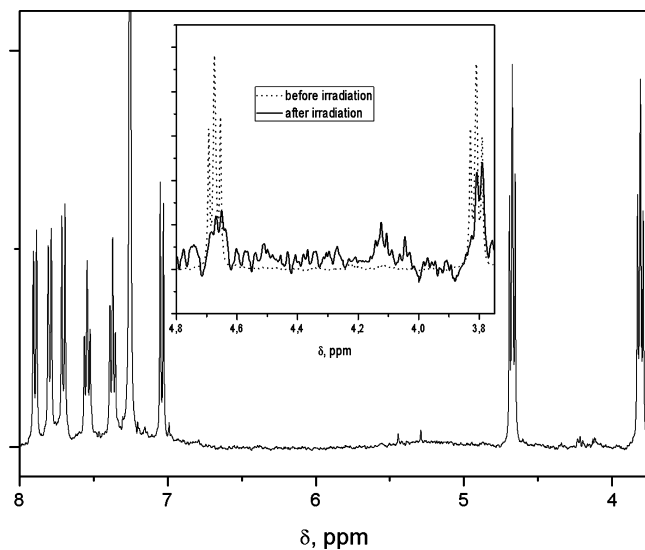


Figure 2. NMR spectra of NO₂nH. (Inset) Alkyl region of the NMR spectra before and after 1 min irradiation with a low-pressure halogen lamp at 254 nm.

corresponding to benzylic protons centered at 3.80, and the triplet at 4.67 assigned to the protons of the carbon α to the nitro group.

Figure 3A presents the absorption spectra of NO₂nH at different pH values. NO₂nH is mostly present in the neutral form at pH ≤ 7 . Two ionization constants were measured, with pK_{a1} 9.7 and 11.6, corresponding to the loss of one and two protons, respectively, in 2% MeOH/H₂O. In view of the expected similarity between the pK_{a} s of naphthol and 2-phenyl-1-nitroethane, the lower pK_{a} corresponds to an anion exchanging a proton between the naphtholate and the carbanion. The second ionization of this species requires a high pH. Figure 3B shows that the ratio of fluorescence intensities $^*RO^-/^*ROH$ of NO₂nH at pH 7.2 is only 0.75, much lower than the value of 2 measured for 1-propyl-2-naphthol.²⁵ Assuming that the radiative and nonradiative decay rates of 1-propyl-2-naphthol and NO₂nH are identical, and that the decay rates in the corresponding anions differ from each other only because of the presence of the nonadiabatic intramolecular proton transfer rate constant (k_{ipt}) in NO₂nH, we can write

$$\frac{k_F^1 + k_{nr}^1 + k_{ipt}}{k_F^1 + k_{nr}^1} = \frac{2}{0.75} \quad (7)$$

and conclude that 63% of the $^*RO^-$ fluorescence quenching is due to the acidic proton of the nitroalkane moiety.

The enhanced quenching of $^*RO^-$ fluorescence in NO₂nH versus 1-propyl-2-naphthol, analyzed above, indicates that the efficiency of intramolecular proton transfer is $\phi_{H^+} \approx 0.63$. The proton comes from the acidic carbon of the nitroalkane moiety, and this efficiency is also the efficiency of carbanion formation. In order to obtain the quantum yield of carbanion formation, we also need to know the $^*RO^-$ formation quantum yield in NO₂nH. At pH 11.9 (only anionic species present) $^*RO^-$ must be formed with a unit quantum yield. As shown in Figure 3B, the emission intensity of the $^*RO^-$ band at 420 nm decreases by a factor of 2.1 as the pH decreases from 11.9 to 7.2 (only neutral species). At pH 7.2 $^*RO^-$ is formed via NO₂nH excitation and deprotonation, and we can assign its fluorescence intensity decrease to the formation of a smaller quantity of $^*RO^-$

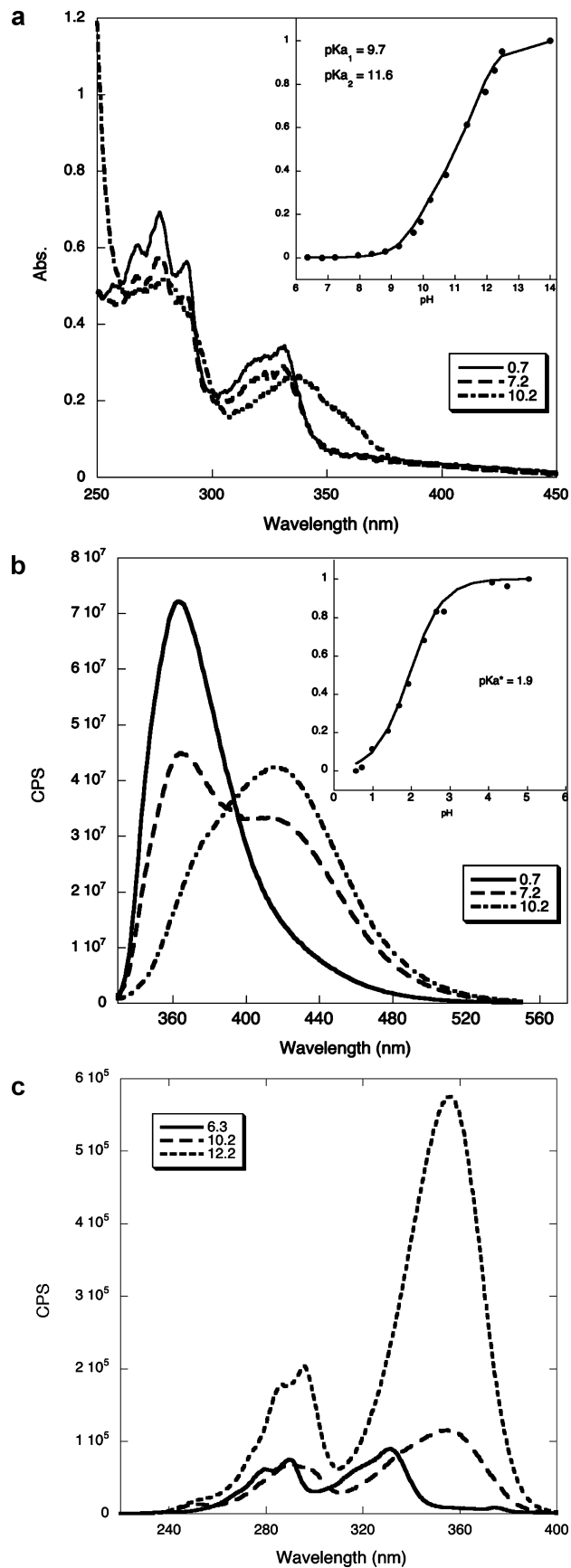


Figure 3. Spectroscopic characterization of NO₂nH; (A) Absorption, (B) Fluorescence and (C) fluorescence–excitation spectra at the indicated pH values in 2% MeOH/H₂O. The insets in (A) and (B) report pK_{a1} and pK_{a2}^* measurements, respectively.

due to the presence of decay mechanisms in *ROH that are competitive with proton transfer to the solvent. Following this reasoning, the decrease in fluorescence intensity gives the $^*RO^-$ formation quantum yield $\Phi_{^*RO^-} \approx 0.48$. The carbanion formation quantum yield is then $\Phi_C = \Phi_{H^+} = \phi_{H^+} \Phi_{^*RO^-} \approx 0.3$. With such a high quantum yield, even under very mild experimental conditions (laser energy of 3 mJ/pulse at 266 nm, 5–6 ns laser pulse width, photoacid absorbance $A_{266} = 0.4$, irradiated volume of 0.1 mL) an aqueous solution initially at pH 7 should acidify to pH 5 within the laser pulse and return to neutrality in one second.

The predominant species in the 8–11 pH range is a monoanion, with the proton located either in the oxygen atom of the naphthol or in the carbon atom at the α position to the nitro group. Carbanions of nitroalkanes may delocalize part of the charge to the adjacent nitro group and resemble a nitronate anion.³² This is an intrinsic property of nitroalkanes and an integral part of their characteristic proton transfer reactions, but only the C-protonation drives the system to its minimum energy and is the reaction coordinate of interest to this work. In view of the calculated intramolecular proton transfer rate and of the similarity between the pK_a s of naphthol and 2-phenyl-1-nitroethane, both the naphtholate and the carbanion forms are present in equilibrium in the ground state. The absorption spectra at pH 10.2 and 11.9 reflect the change from a mono to a dianion, but do not inform on the spectral properties on the two monoanions. Fluorescence excitation spectra of Figure 3C suggest that the band near 350 nm corresponds to the naphtholate form of the anion.

Other mechanisms may be invoked for the quenching of $^*RO^-$ fluorescence in NO₂nH. However, we can exclude solvation effects, because the presence of hydroxyl groups in the alkyl chain increases the intensity of the anion emission,²⁵ whereas we observe a decrease in fluorescence intensity in the presence of the nitro group. The fluorescence decays obtained at the emission maxima of *ROH (360 nm) and $^*RO^-$ (430 nm), measured by single-photon counting and shown in Figure 4, are not amenable to a simple interpretation because geminate recombination leads to nonexponential behavior.³³ Nevertheless, the decay of $^*RO^-$ gives a good fit to an exponential decay with a time constant $k_{^*RO^-} = 1.4 \times 10^8 \text{ s}^{-1}$ which, after subtraction of the decay constant measured for the anion of 1-propyl-2-naphthol,²⁵ gives $k_{ipt} \approx 10^8 \text{ s}^{-1}$ in 2% MeOH:H₂O. This is in excellent agreement with the rate constant $k_{ipt} = 2.6 \times 10^8 \text{ s}^{-1}$ anticipated with ISM.

Direct evidence for the formation of a long-lived monoanion upon electronic excitation of NO₂nH, is presented in Figure 5. Excitation at 266 nm of 0.1 mM of NO₂nH in 2% MeOH/H₂O initially at pH 7 produces a transient absorption spectrum with bands at 315 and 355 nm with similar decays. The spectra were collected at sufficiently long times to ensure that any naphtholate formed directly from its excited state is already reprotonated back to the neutral form of NO₂nH. Considering that the rate of formation of the naphtholate from the carbanion is much slower than the rate of protonation of the naphtholate, we assign the spectra in Figure 5A to the carbanion. The reestablishment of Equilibrium (5) is characterized by a relaxation time, defined as the time at which the distance from equilibrium is $1/e$ of the initial distance. The relaxation time can be extracted from the

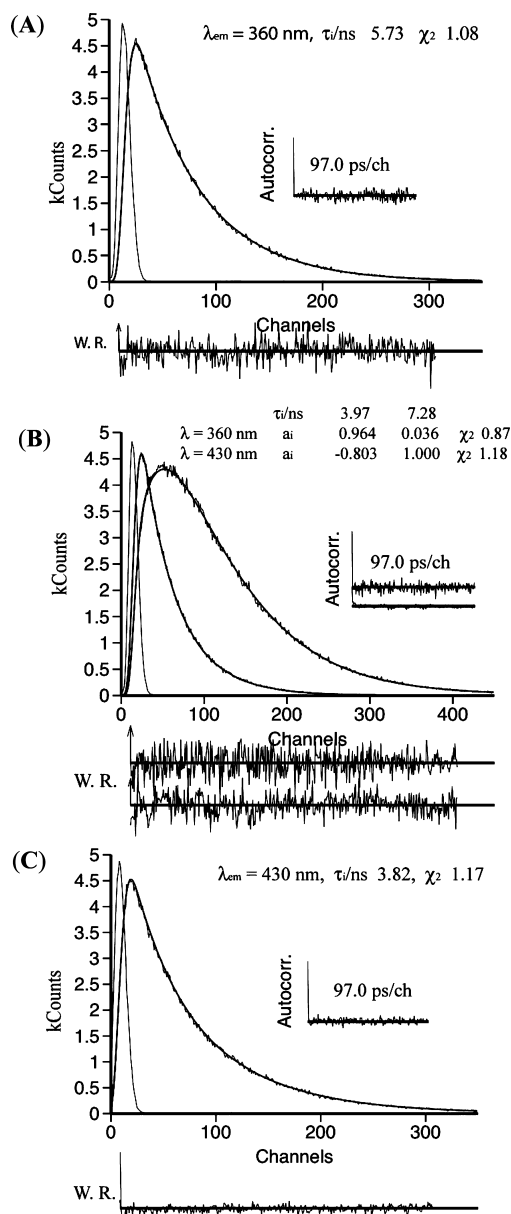


Figure 4. Single photon counting of 1-(2-nitroethyl)-2-naphthol. (a) At pH 1.0. (b) At pH 6.4. (c) pH 12.2.

experimental data as shown in Figure 5B. The value obtained, $\tau \approx 0.6 \text{ s}$, is in remarkable agreement with the relaxation time predicted by theoretical modeling of this system, 1 s. We can classify this pH jump as “persistent” in the perspective of all the processes that occur in millisecond and submillisecond regimes and that cannot be studied by rapid-mixing techniques.

Definitive evidence for the mechanism of Figure 1 can be obtained with photolysis in 2% MeOD/D₂O, which must lead to the incorporation of deuterium in NO₂nH. The inset in Figure 2A shows the NMR spectra of NO₂nH collected before and after 1 min photolysis in 2% MeOD/D₂O with a mercury lamp at 254 nm. The compound was extracted with CDCl₃ and the NMR spectra were registered in this solvent. The triplet assigned to the protons next to the nitro group decreases in intensity, as expected from the protonation of the carbanion by D₃O⁺. At the same time, the benzylic protons become a doublet because the coupling is now with only one proton. Potassium ferrioxalate actinometry reveals that 9×10^{-5} moles of photons were absorbed and 9×10^{-7} moles of photoacid were present. The

(32) Erden, I.; Keefe, J. R.; Xu, F.-P.; Zheng, J.-B. *J. Am. Chem. Soc.* **1993**, *115*, 9834–9835.

(33) Agmon, N.; Huppert, D.; Masad, A.; Pines, E. *J. Phys. Chem.* **1991**, *95*, 10407–10413.

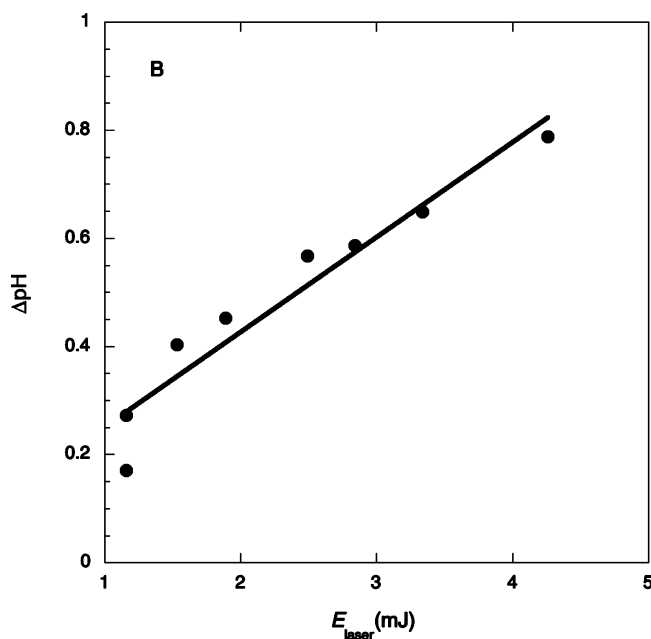
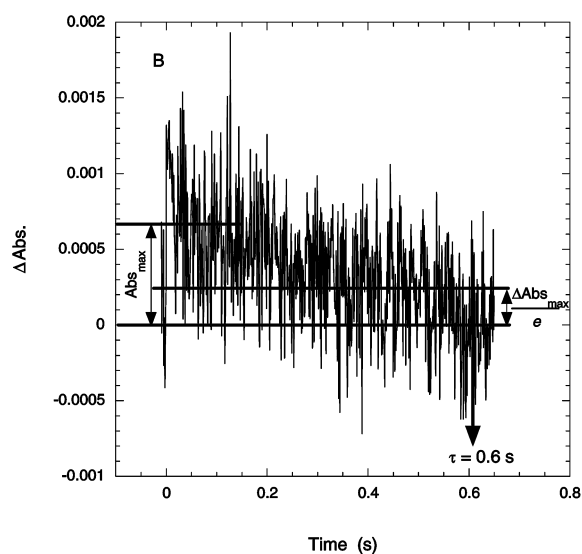
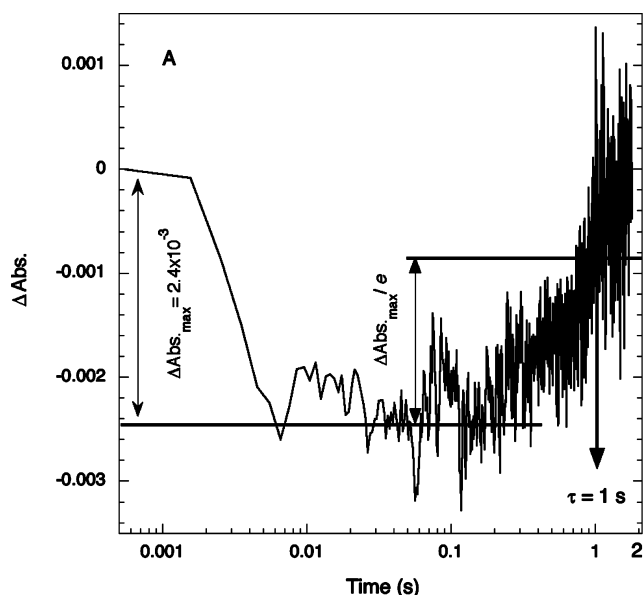
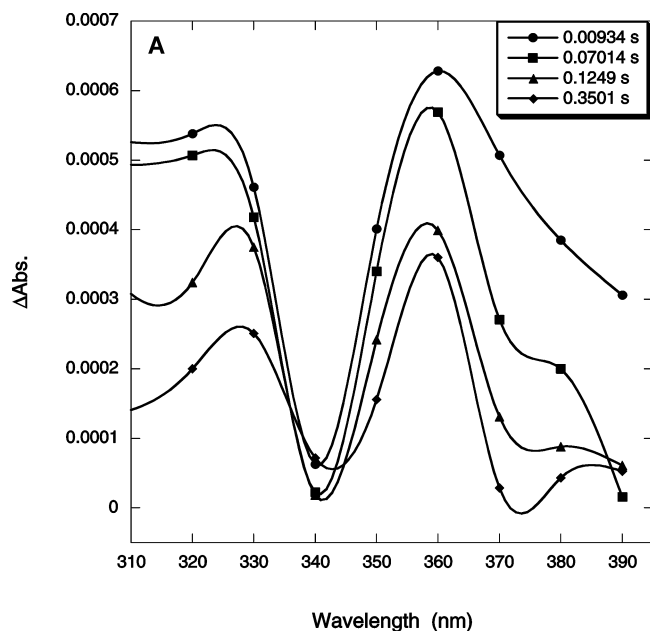


Figure 5. Flash photolysis of $[\text{NO}_2\text{nH}] = 4.3 \times 10^{-4} \text{ M}$ in 2% MeOH: H_2O . (A) Transient absorption spectra. (B) Decay at 360 nm.

Figure 6. Transient bromocresol green absorption at 616 nm following flash photolysis of $[\text{NO}_2\text{nH}] = 2 \times 10^{-4} \text{ M}$ in 2% MeOH/ H_2O . (A) Bleaching and recovery of bromocresol green absorption with estimate of the relaxation time τ . (B) Dependence of the maximum photobleaching of bromocresol green on the laser intensity; the slight offset of the laser energy is probably due to some 355 nm stray light reaching the energy meter. No photobleaching is observed in the absence of NO_2nH .

excess of protons released should lead to 100% deuteration of NO_2nH . The NMR spectra show that this extensive deuteration is not accompanied by significant degradation. Moreover, detailed analysis of the aromatic region of the NMR spectra reveals that incorporation of deuterium in the α position of the nitro group is not accompanied by changes in the aromatic protons. Thus, we conclude that our persistent photoacid is also reversible.

The data above proves the success of the design of persistent and reversible photoacids that employ competitive intramolecular proton transfer from a carbon acid. The amplitude of the pH jump in such systems is limited by the acidity of the photoacid ($\text{p}K_a^* = 1.5$ from fluorescence titration), by its solubility and by the intensity of the laser pulse. The color change of pH indicators is a very convenient tool to assess the amplitude of the pH jump and the availability of the excess protons to participate in chemical reactions. We employed bromocresol green ($\text{p}K_a = 4.9$) and observed the bleaching and recovery of its basic form (In^{2-}) at 616 nm, where the absorption

coefficient is $\epsilon_{616} = 39550 \text{ M}^{-1} \text{ s}^{-1}$. Figure 6A shows that the absorbance change produced by a 3 mJ laser pulse 2 mm in diameter in a 2% MeOH/ H_2O solution with initial indicator concentration $[\text{In}^{2-}] = 9.1 \times 10^{-6} \text{ M}$ at pH 7, is $\Delta A_{616} = -2.4 \times 10^{-3}$. This absorbance change corresponds to $\Delta[\text{In}^{2-}] = 3 \times 10^{-7} \text{ M}$ and a jump to pH 6.3. This is a conservative estimate given the geometric mismatch between the analyzing light beam and the laser flash. A more realistic estimate is that the lowest pH attained with this 3 mJ laser pulse is between the theoretical estimate of pH 5 and the experimental evidence for pH 6. More importantly, as shown in Figure 6B, is that the magnitude of the pH jump is directly proportional to the laser energy. With

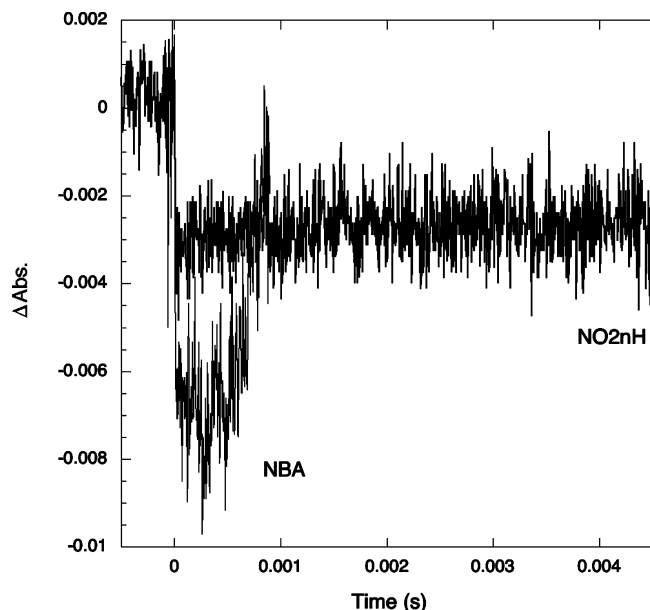
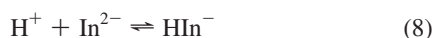


Figure 7. Transient bleaching of bromocresol green absorption at 616 nm following flash photolysis of $[\text{NO}_2\text{nH}] = 2 \times 10^{-4}$ M or of $[\text{NBA}] = 4 \times 10^{-3}$ M in 2% MeOH:H₂O. The initial pH was 5.2 and the indicator concentration was 1.2×10^{-5} M for NO₂nH and 2.5×10^{-6} M for NBA experiments.

intense laser pulses, the proton concentration should approach the solubility limit of NO₂nH.

The acid–base recombination rate constant of bromocresol green is $k_{\text{on}} = 5.8 \times 10^{10} \text{ M}^{-1} \text{ s}^{-1}$,³⁴



and the ionization rate constant is $k_{\text{off}} = 6.8 \times 10^5 \text{ s}^{-1}$. Both these rates are much faster than the corresponding ones for Equilibrium (5), which means that the acid and basic forms of bromocresol green are in equilibrium at the medium pH all along the recovery of the system to neutrality. Thus, the rate-determining factor for the recovery of bromocresol green is the bimolecular reprotonation of the carbanion, and the relaxation time of $[\text{In}^{2-}]$ should be the same as that of the carbanion. Figure 6A shows that the relaxation time of bromocresol green is $\tau = 1$ s, which is the same within experimental error as that of the carbanion in Figure 5B. This experiment shows that the protons generated in the irradiated volume establish new equilibria in the submillisecond time scale and that pH-dependent equilibrium concentrations in that regime can be followed directly.

The breakthrough in the pH jump technique made possible by NO₂nH can be best appreciated comparing its persistent and reversible pH jump with the pH jump produced by the most common caged proton compound, *o*-nitrobenzaldehyde (NBA),³⁵ under similar conditions, Figure 7. NBA is capable

of pH jumps lasting for seconds when the initial pH is close to 7. However, in our experiments with pH 5.2, adjusted with HCl, the pH jump produced with NBA is quenched in milliseconds presumably as a result of reactions of the NBA product. Terazima observed a similar effect and concluded that experimental results utilizing caged compounds must be carefully analyzed in view of the possible reactions of NBA photoproducts, namely with Cl⁻.³⁶

5. Conclusions

The design and synthesis of a persistent and reversible photoacid was motivated by theoretical modeling, and is another illustration of scientific advances driven by theory. The synthesis of 1-(2-nitroethyl)-2-naphthol was achieved by a simple two step procedure, that allows the isolation of the desired product without requiring chromatographic separations and is a valid starting point for scale-up procedures.

In aqueous solutions, deprotonation of 1-(2-nitroethyl)-2-naphthol is essentially completed in 10 ns, and leads to a carbanion located at the α position to the nitro group with a ca. 30% efficiency. The relaxation time for the reprotonation of this carbanion, and the consequent return to neutrality, is close to 1 s. Thus, from 10 ns to 0.1 s, the irradiated volume remains acidic and at a nearly constant pH. This offers a simple method to study pH-dependent processes that are faster than the time resolution of rapid-mixing techniques.

The flash photolysis data was collected as an average of 5 laser pulses with laser repetition rates below 0.2 Hz. Each laser shot produces a similar transient spectrum, and the baseline fully recovers before the next shot. The pH jumps corresponding to the on–off light cycles are highly reproducible. Pure samples can be subject to hundreds of laser pulses without appreciable spectral changes. NO₂nH is the first example of a persistent and reversible photoacid and proves the feasibility of this concept.

Finally, it must be emphasized that these photoacids offer a local control of acidity and that while diffusing a few micrometers from the irradiated volume, the carbanion is neutralized.

Acknowledgment. This work was supported by FCT and FEDER (project no. POCI/QUI/55505/2004). R.M.D.N. thanks FCT for the grant SFRH/BD/24005/2005. We thank the Nuclear Magnetic Resonance Laboratory of the Coimbra Chemistry Centre for obtaining the NMR data.

Supporting Information Available: ¹H NMR and ¹³C NMR. Input and output files for ISM calculations through the Internet, together with the explanation of the terms employed. This material is available free of charge via the Internet at <http://pubs.acs.org>.

JA901930C

(34) Warrick Jr., P.; Auburn, J. J.; Eyring, E. M. *J. Phys. Chem.* **1972**, *76*, 1184–1191.

(35) Viappiani, C.; Bonetti, G.; Carcelli, M.; Ferrari, F.; Sternieri, A. *Rev. Sci. Instrum.* **1998**, *69*, 270–276.

(36) Choi, J.; Terazima, M. *J. Phys. Chem. B* **2003**, *107*, 9552–9557.